JGR Biogeosciences

RESEARCH ARTICLE
10.1029/2023JG007480

Lipid Biosignatures From SO_4-Rich Hypersaline Lakes of the Cariboo Plateau

Floyd Nichols[1], Alexandra Pontefract[2], Hannah Dion-Kirschner[1,3], Andrew L. Masterson[1,4], and Magdalena R. Osburn[1]

[1]Department of Earth and Planetary Sciences, Northwestern University, Evanston, IL, USA, [2]Space Exploration Sector, Johns Hopkins University Applied Physics Laboratory, Laurel, MD, USA, [3]Now at Division of Geological and Planetary Sciences, California Institute of Technology, Pasadena, CA, USA, [4]United States Geological Survey, Reston, VA, USA

Key Points:

- SO_4-dominated hypersaline lakes produce more abundant organic matter (OM) than a Na_2CO_3-dominated site of comparable salinity
- The circumneutral $MgSO_4$-dominated hypersaline lakes studied here harbor abundant microbial biosignatures compared to other Martian analogs
- Lipid biosignatures produced in situ predominate within sedimentary OM rather than biosignatures produced by surrounding vegetation

Correspondence to:

F. Nichols and M. R. Osburn,
floydnichols2025@u.northwestern.edu;
maggie@northwestern.edu

Citation:

Nichols, F., Pontefract, A., Dion-Kirschner, H., Masterson, A. L., & Osburn, M. R. (2023). Lipid biosignatures from SO_4-rich hypersaline lakes of the Cariboo Plateau. *Journal of Geophysical Research: Biogeosciences*, *128*, e2023JG007480. https://doi.org/10.1029/2023JG007480

Received 13 MAR 2023
Accepted 15 SEP 2023

Abstract Modern and ancient hypersaline brines have been identified across the solar system, but the habitability of these environments remains unknown. Here, we evaluate organic matter (OM) production in $MgSO_4$ and Na_2CO_3 rich hypersaline lakes whose chemistries resemble deposits on Mars such as those identified in Jezero crater. We focus our analysis on lipid biomarkers including fatty acids, alkanes, and ether-bound lipids in modern brines, salt deposits, and surface sediments. We also report total organic carbon (TOC), carbon/nitrogen (C/N) ratios, and bulk OC ($\delta^{13}C$ and $\delta^{15}N$) isotopes to contextualize the lipid biomarker data. In all lakes, the predominant biosignatures include midchain ($12 < C < 23$) fatty acids and alkanes suggesting microbial origin. Sediments also incorporate a greater diversity of lipids. Ether-bound lipids derived from archaea and bacteria constitute a minor but measurable fraction of the lipids. This result contrasts with typical findings from other studies with NaCl brines which contain significant archeal biomass. TOC concentrations in all sediments are high, ranging from 0.7% to 12% with sulfate-rich sediments having the highest concentrations. The isotopic and elemental compositions of TOC corroborate the biomarker results, showing $\delta^{13}C$ values and C/N values indicative of aquatic microbial origin. This richness of organic matter and in situ microbial biosignatures differ from previously studied Cl-dominated Mars-analog sites which have shown limited OM production and preservation and acidic SO_4-rich hypersaline environments which were dominated by terrestrial inputs. Overall, our results suggest that $MgSO_4$-rich hypersaline environments are conducive for life and harbor a rich microbial biomarker landscape.

Plain Language Summary The minerals found on Mars suggest that it had abundant hypersaline waters early in its history. However, liquid water no longer persists on its surface. As such, we must use environments on Earth that are similar to Mars and other astrobiological targets to better understand the potential for life elsewhere. Here, we examine fatty molecules and organic carbon from hypersaline lakes on Earth that resemble water compositions thought to have been present on early Mars. We also use bulk carbon isotopic data to help inform the results from our biomarker analysis. Overall, data from these sites shows that circumneutral SO_4-rich environments are conducive for life and harbor a suite of microbial biosignatures. In comparison to other Martian-analog environments on Earth, this study shows that circumneutral SO_4-dominated lakes produce in situ biological signatures in abundance.

1. Introduction

Detection of past or extant life beyond Earth is a primary driver of mission-based planetary science. As life detection efforts push forward, an emphasis on habitability is imperative (Kite et al., 2018). Previous work on extreme environments on Earth have identified environmental parameters that may limit habitability such as evidence for syndepositional desiccation, perchlorate salts, acidic fluids, and/or hypersaline fluids (Carrizo et al., 2019; Hallsworth et al., 2007; Wilhelm et al., 2017). In hypersaline environments specifically, habitability is affected by ionic strength (concentration of ions in solution), water activity (a_w, thermodynamic availability of water), and lyotropic properties (ion specific behavior in aqueous solutions) of solutes (Fox-Powell et al., 2016; Pontefract et al., 2017). These factors ultimately govern the production and stability of organic matter (OM) and biosignatures found in resultant deposits. Most hypersaline lakes on Earth are dominated by NaCl where the Cl^- anion is chaotropic or membrane destabilizing (Hallsworth et al., 2007; Pontefract et al., 2017). Additionally, many Mars-analog hypersaline lakes that are Cl-dominated are paired with the Ca^{2+} or Mg^{2+} cation (e.g., Don Juan Pond in Antarctica, the Discovery Basin in the Mediterranean, and the South Bay Salt Work Bitterns in Southern

California) which can be highly chaotropic solutes depending on the organic molecule in question (Dickson et al., 2013; Fisher et al., 2021; Hallsworth et al., 2007; Klempay et al., 2021). For instance, the low charge density of Cl^- causes it to destabilize proteins and inhibit cellular functions by adsorbing to cationic nitrogen-based amino acid chains, ultimately, decreasing protein hydration and stability (Collins, 1997; Fisher et al., 2021). Conversely, the charge density of SO_4^{2-} promotes hydration and stabilizes proteins (Collins, 1997; Fisher et al., 2021; Hallsworth et al., 2007). Despite different methodologies, which can be compared semi-quantitatively, work done using 16S rRNA analysis (Hallsworth et al., 2007; Klempay et al., 2021) and lipid biomarker analysis (Carrizo et al., 2019; Wilhelm et al., 2017) has shown that these sites contain some of the lowest biomass levels found on Earth, with correspondingly low microbial diversity and organic content. While these studies are informative, many of these sites resemble modern-day Martian environments rather than those that encompass conditions present deeper in its history (Ehlmann et al., 2008). The viability of life and production of biosignatures by other environments with ions that are kosmotropic or membrane stabilizing such as SO_4^{2-} remain poorly constrained (Fox-Powell & Cockell, 2018; Hallsworth et al., 2007; Pontefract et al., 2017; Tosca et al., 2008).

Extremely SO_4-rich aqueous environments are rare on Earth yet key astrobiological targets on Mars because they host ancient evaporite deposits comprised of SO_4 and Mg-rich salts (Aubrey et al., 2006; Fox-Powell & Cockell, 2018; Pontefract et al., 2017; Tosca et al., 2008). Environments with these fluid chemistries are known on Earth from South-Central British Columbia and Western Australia which each host a variety of such systems (Johnson et al., 2020; Pontefract et al., 2017). Previous work on these Mars-analog environments has shown a range of OM production, preservation, or microbial activity. Work done using metagenomic analysis in Spotted Lake (South-Central British, Columbia), a circumneutral Mg-SO_4 lake, showed the microbial community to be quite diverse and abundant (Pontefract et al., 2017). Lipid biomarkers are key tools to understand the astrobiological potential of these environments, due to their specificity to life and ability to be preserved on long geologic time scales (Brocks & Pearson, 2005; Johnson et al., 2018). Analysis of lipid biomarkers in acidic sulfate-rich lakes including Lake Gneiss and Lake Gilmore (Western Australia) showed very low biomass, diversity, and microbial lipid preservation (Johnson et al., 2020). Although these lakes are saturated with $MgSO_4$, the acidic conditions likely contributed to the very low concentrations of microbial lipids, especially short saturated and branched fatty acids. The dominant lipid signatures within the sediments were long chain *n*-alkanes and fatty acids, reflecting the selection of terrestrial vegetation inputs.

There remains a knowledge gap surrounding the habitability of circumneutral to alkaline SO_4-dominated hypersaline Mars analog environments, as few studies target these systems (Fox-Powell & Cockell, 2018; Pontefract et al., 2017) and even fewer have probed their production potential of OM and lipid biosignatures (Benison & Karmanocky, 2014; Johnson et al., 2020). Results thus far are promising. For instance, Cheng et al. (2017) observed bacterial and archeal lipids in terrestrial SO_4 salts and microorganisms such as diatoms and algae have been described from within fluid inclusions of gypsum ($CaSO_4 \cdot 2H_2O$; Benison & Karmanocky, 2014). Constraining the production potential of OM in terrestrial SO_4 and Mg-rich hypersaline lakes is necessary to inform the search for extraterrestrial life due to their kosmotropic potential. Here, we evaluate the production potential of OM in the kosmotropic Mars analog hypersaline lakes of the Cariboo Plateau, British Columbia, using a lipid biomarker and isotope organic geochemistry approach.

2. Site Description

The lakes targeted here are situated on the Cariboo Plateau of South-Central Interior British Columbia, Canada, between the Coast and Columbia-Rocky mountain ranges. Numerous lakes formed in this region ~10,000 years ago as glacial retreat produced closed basins with limited drainage (Pontefract et al., 2017; Renaut & Long, 1989). Most of these lakes, including those studied here, are principally groundwater-fed, with additional contributions from precipitation (Renaut, 1990; Renaut & Long, 1989). This region is situated in the rain shadow of the Coast Mountains producing a semi-arid to sub-humid climate with an average annual precipitation of 300–400 mm yr^{-1} (Renaut & Long, 1989). The region also experiences extreme annual temperature ranges with average daily highs up to 35°C in the summer, and temperatures as low as −40°C in the winter (Renaut, 1993). These conditions produce ephemeral lakes that dry completely. Our three focus areas include the Basque Lakes (Basque Lake #1: 50°36′1.8″ N, 121°21′32.4″ W, Basque Lake #2: 50°35′36.6″ N, 121°20′58.2″ W, and Basque Lake #4: 50°35′20.304″ N, 121°20′34.397″ W), Clinton (Salt) Lake: 51°04′25.44″ N, 121°35′11.244″ W, and Last Chance Lake: 51°19′40.8″ N, 121°38′9.6″ W (Figure 1). The chemical compositions of the brines in these systems are

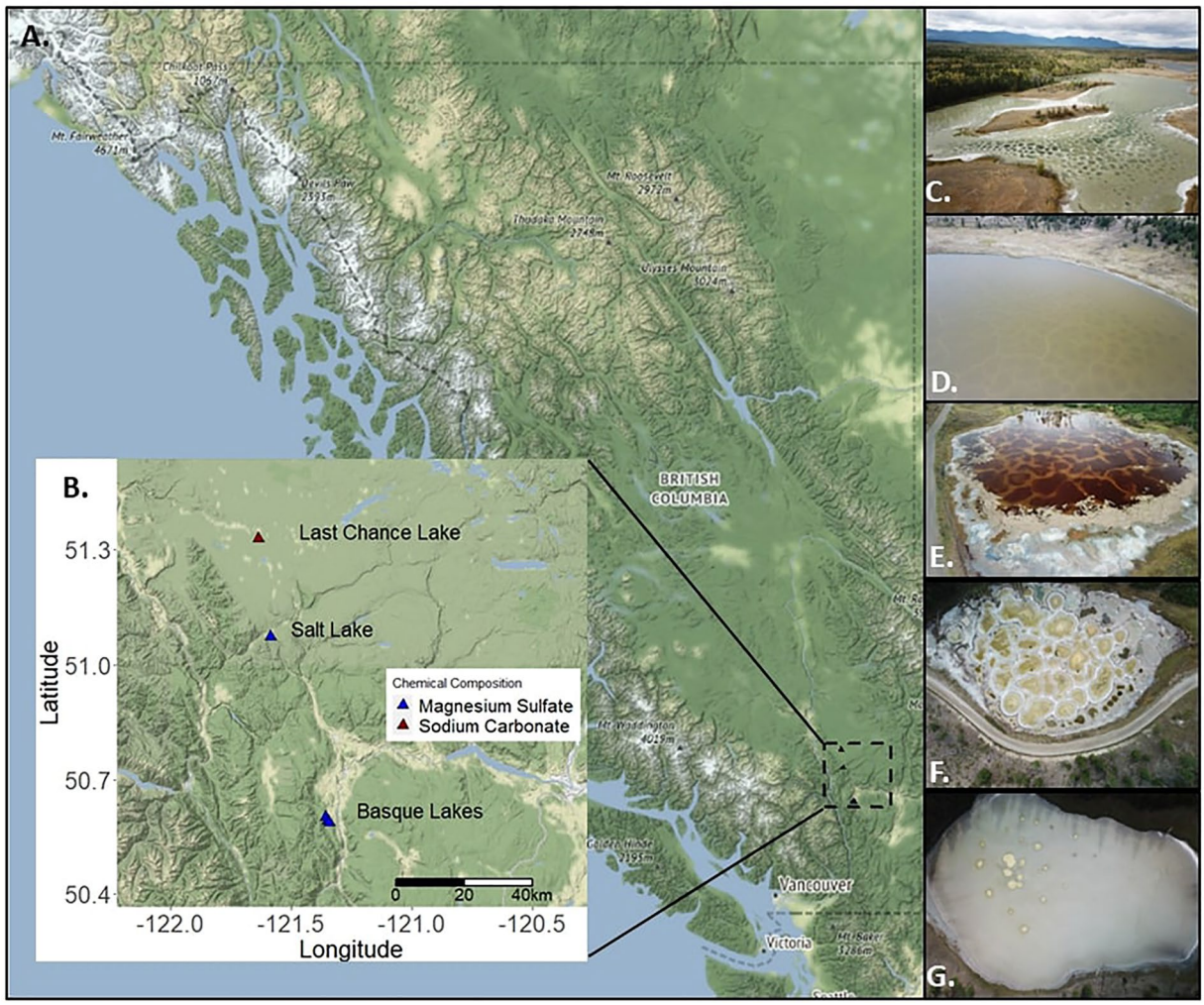

Figure 1. Map of study site. (a) Province of British Columbia, Canada and (b) inset of part of the Cariboo Plateau. Aerial photographs of the lakes studied: (c) Last Chance Lake: 51°19′40.8″ N, 121°38′9.6″ W, diameter ~680 m. (d) Salt Lake: 51°04′25.44″ N, 121°35′11.244″ W, diameter ~380 m. (e) Basque Lake #1: 50°36′1.8″ N, 121°21′32.4″ W, diameter ~200 m. (f) Basque Lake #2: 50°35′36.6″ N, 121°20′58.2″ W, diameter ~160 m. (g) Basque Lake #4: 50°35′20.304″ N, 121°20′34.397″ W, diameter ~170 m. Photo credit: Mitchell Barklage. Map created using the package ggmaps in R.

controlled by groundwater mediated bedrock dissolution: the Basque Lakes and Salt Lake are underlain by greenschist facies, and Paleozoic-Mesozoic metasediments of the Chilcotin Group (Salt Lake) respectively, and Venables Valley assemblage (Basque Lakes), including abundant localized pyrite deposits, whereas Na-CO_3-SO_4-Cl rich lake (Last Chance Lake) is underlain by basalts of the Chilcotin Group and surficial glacial sediments (Cui et al., 2017; Renaut & Long, 1989). As a result of this, high levels of Mg^{2+} and SO_4^{2-} are present in the groundwater and are concentrated to saturation through evaporation during the summer months.

The lakes in this study are also unique in the world, featuring a distinctive "spotted" appearance with numerous separate but adjoining brine pools forming within each basin (Figure 1; Pontefract et al., 2017; Renaut, 1990; Renaut & Long, 1989; Jenkins, 1918). The origin and structure of these spots is a matter of debate (Renaut, 1990) and is being investigated as part of our ongoing research. Despite the aridity, heavily vegetated catchment areas surround many of these lakes featuring conifer forests and grassland assemblages, indicating that aridity is not an impedance.

3. Materials and Methods

3.1. Sampling

We sampled water, surface sediment, microbial mats and salt deposits from the Basque Lakes, Salt Lake, and Last Chance Lake in summer 2018, winter 2019, and summer 2019. Physicochemical measurements of the brines

including pH, total dissolved solid (TDS), temperature, oxidation reduction potential (ORP), and conductivity were measured before sample collection using both a portable YSI probe and a Hanna Multiparameter Meter. Water activity was measured on-site using an AquaLab 4TE water activity dew point meter, with temperature control. Brine samples were collected for ionic composition, dissolved organic carbon (DOC), water isotopic composition, and dissolved inorganic carbon (DIC). Samples for ionic composition were analyzed by ACZ labs in Steamboat Springs, CO. A subset of redox sensitive ions ($\sum S^{2-}$, Fe^{++}, NO^{-}_{3}, NH^{+}_{4}) were measured in the field using a Hach Spectrophotometer via established protocols (Osburn et al., 2014). DOC was quantified by Anatek labs in Spokane, WA.

Particulate Organic Matter (POM—primarily cells) was filtered from water for lipid analysis through 90 mm pre-combusted 0.3 μm glass fiber filters using a field peristaltic pump (Geotech). Filters were wrapped in pre-combusted foil and frozen until analysis. In winter 2019, POM from samples of lake ice were also collected by melting ice chunks in field-rinsed buckets then collecting POM on filters as described above. Microbial mats, salt deposits, and sediments for lipid extraction were collected using solvent-rinsed tools into pre-combusted soil jars from multiple places in each lake or brine pool. Surface sediment samples included only the top 3 cm of sediment. All samples for lipid analysis were frozen within 6 hr of collection, transported frozen to the lab, and stored at −20°C until further processing.

3.2. Total Organic Carbon and Stable Isotope Analysis

The carbon and nitrogen stable isotopic composition of bulk OM (sediments/salts/mats) and POM (brines), as well as TOC and TON concentrations were measured in the Northwestern Stable Isotope Biogeochemistry Lab with an elemental analyzer isotope ratio mass spectrometer (EA-IRMS; Costech 4010 EA coupled to a Thermo Delta V+IRMS through a Conflo IV interface). Freeze-dried samples were weighed then were treated with 1M HCl to remove inorganic carbon and acid soluble salts, rinsed with MilliQ water, then freeze-dried and weighed again. The homogenized sample was loaded into tin capsules for analysis. Standards were run every 10 samples including IU-acetanilide ($\delta^{13}C = -29.5$ ‰, $\delta^{15}N = 1.2$ ‰) and urea ($\delta^{13}C = -8.0$ ‰, $\delta^{15}N = 20.2$ ‰). Carbon isotopes are reported with respect to Vienna Pee Dee Belemnite (VPDB) and nitrogen isotopes are reported with respect to atmospheric N_2 (AIR; Schimmelmann et al., 2009).

3.3. Lipid Extraction

Frozen samples were freeze-dried and homogenized using a solvent-rinsed mortar and pestle. Lipids were extracted from each sample using a modified Bligh and Dyer (Bligh & Dyer, 1959) method according to Johnson et al. (2018). In brief, three to six g of homogenized sample (sediments, salts, and microbial mats) or an entire POM filter (brines) was sonicated with a single-phase mixture of methanol (MeOH), dichloromethane (DCM), and aqueous buffer (2 × 50 mM dibasic potassium phosphate, 2X trichloroacetic acid) mixture, centrifuged, and combined. Additional DCM and water were added to form a two-phase solution of which the organic fraction was collected. Elemental sulfur was removed from the lipid extracts by reaction with activated and triple solvent-rinsed copper granules (if elemental sulfur was present copper granules turned dark). Samples were then split for ester-bound lipid analysis and ether-bound lipid analysis. Ester-bound lipids were liberated by base saponification with 0.5 M NaOH heated at 70°C for 16 hr. Saponification reactions were acidified, then the organic fraction was extracted with 10 mL of methyl tert-butyl ether three times and dried. To liberate ether-bound core lipids, the method described by Kaneko et al. (2011) was employed. In brief, 0.5 mL of hydroiodic (HI) acid was added to dry lipid extracts, purged with a stream of N_2 gas, and heated at 120°C for 4 hr. Once cooled, 1 ml of clean water and 2 mL hexane were added to the HI and shaken vigorously to extract the cleaved products.

3.4. Lipid Separation and Derivatization

Hydrolyzed ester-bound lipids were separated into four fractions: alkane (4 mL of hexane), ketone (7 mL of 4:1 hexane:DCM), alcohol (7 mL of 9:1 DCM:acetone), and fatty acid (8 mL of 2.5% formic acid in DCM) with aminopropyl substituted solid-phase extraction columns (Supelco, Discovery DSC-NH_2). Alcohol fractions were derivatized to acetate esters with pyridine and acetic anhydride, heated at 70°C for 20 min. Fatty acids were derivatized to methyl esters (FAMEs) with 12.5% Boron Trifluoride (BF_3) in anhydrous MeOH and heated at 70°C for 10 min, followed by extraction with hexane (3X) and removal of water with Na_2SO_4. Ether-bound lipids were

subjected to a hydrogenation reaction to reduce alkyl iodides. The cleaved ether products was combined with 5 mg of platinum oxide (PtO_2) under a stream of H_2 gas and stirred between 800 and 1,000 rpm for 90 min. Data from alkanes, fatty acid, and ether-bound fractions are discussed here.

3.5. Biomarker Quantification and Identification

Biomarkers were identified and quantified using gas chromatography-flame ionization detection-mass spectrometry (GC-FID-MS) with a ThermoFisher Trace GC 1310 coupled to an FID and ISQ quadrupole MS. A Zebron ZB-5 capillary GC column (30 m × 0.25 mm × 25 μm) was used to separate ester-bound compounds with He carrier gas at 1 ml/min. For each separated hydrolyzed ester-bound lipids, 2 μL was injected into a PTV injector (70°C initial, evaporated at 100°C for 1 min). The GC oven temperature schedule for ester-bound lipids was as follows: 1 min hold at 100°C, ramped to 320°C at 14°C/min, followed by a final 10-min hold. The MS conditions included ion scanning between 60 and 600 (amu) every 0.2 s. Sample peaks were quantified relative to the intensity of a known quantity of palmitic acid isobutyl ester (PAIBE) added to each sample prior to analysis.

A Zebron ZB-5HT Inferno capillary GC column (30 m × 0.25 mm × 0.25 μm) was used to separate ether-bound compounds with He carrier gas at 1 ml/min. The GC conditions for ether-bound lipids was modeled after (Gattinger et al., 2003). For each sample run, 2 μL was injected into a PTV injector (70°C initial, evaporated at 100°C for 1 min). The GC oven temperature schedule for ether-bound lipids was as follows: Initial temperature at 70°C, ramped to 130°C at 30°C/min, followed by a ramp to 320°C at 10°C/min, and then followed by a final ramp to 350°C at 8°C/min. The MS conditions were the same as above.

3.6. Statistical Analyses and Data Visualization

Statistical analyses were performed to evaluate relationships between samples using the "vegan" package in R (Oksanen et al., 2019). Principal Component Analysis (PCA) was used to reduce data dimensionality and calculate the compositional similarity between sites based on differences in abundance and diversity of lipids. Similarly, hierarchical clustering was performed using the linkage library in Python to create a dendrogram of sites based on lipid distributions using the Ward clustering algorithm. All data was visualized using the ggplot2 package in R (Wickham, 2016) or matplotlib in Python (Hunter, 2007).

4. Results

4.1. Brine Geochemistry

The salinity of the brines ranged from 98 to 327 ppt (9.8%–32.7% salinity). During our study, we observed the highest salinities during the summer 2019 season from the brine pools within Basque Lake #1. The ionic strength of the brines in this study were also exceptionally high ranging from 2.97 to 10.57 (Table 2). Additionally, the water activities of the brines ranged from 0.90 to 0.99. Salt Lake (which did not exhibit distinct brine pools at the time of sampling) and the brine pool (Brine 23) within Basque Lake #2 had the lowest measured salinities. The lowest water activities were from the sub brine pools within Basque Lake #2 and the highest was from Salt Lake. The pH of all lakes was circumneutral to alkaline. The average pH of each site was as follows: Salt Lake, 8.11; Basque Lake #1, 7.86; Basque Lake #2, 8.39; Basque Lake #4, 7.62; and Last Chance Lake, 9.94 (Table 1).

The dominant cations observed here were Mg^{2+} in the Basque Lakes and Salt Lake and Na^{+} in Last Chance Lake (Figure 2). The dominant anions observed were SO_4^{2-} in the Basque Lakes and Salt Lake with Last Chance Lake dominated by HCO_3^{-} and CO_3^{2-} (Figure 2).

4.2. Sediment Geochemistry

Bulk OM concentrations in fluids (measured as mg/mL filtered) and solids (mg/g dry weight) varied between the lakes as well as the sample types (Table 2). TOC for all lakes and sample types ranged from at or below detection limit to 42.8%. The $\delta^{13}C$ values of this organic material ranged from −28.3 to −10.2‰. Total nitrogen (TN) ranged from at or below detection limit to 0.3%. $\delta^{15}N$ values ranged from 1.2 to 14.8‰. Total lipid extract (TLE) concentrations determined gravimetrically ranged from 0.21 to 15.70 mg/g dry sample weight. TLE/TOC, representing the proportion of solvent extractable compounds within the TOC, ranged from at or below detection limit to 55.0 mg TLE per g of organic carbon.

Table 1
Average Geochemistry of the Brines

Lake	Ca	Mg	Na	Cl	SO_4	CO_3	HCO_3	pH	Salinity	Ionic strength	a_w
Basque Lake #1											
Brine 1	0.32	59.35	17.20	1.59	242.50	0.00	1.41	7.92	322.35	10.36	0.91
Brine 2	0.33	61.60	16.50	1.54	244.00	0.22	2.54	7.80	326.70	10.57	0.90
Basque Lake #2											
Brine 1	0.35	40.15	17.90	1.63	198.00	0.00	1.94	8.42	259.65	7.87	0.91
Brine 2	0.36	45.20	19.05	1.51	212.00	0.00	1.17	8.45	279.04	8.60	0.90
Brine 3	0.48	30.50	16.65	0.79	141.20	0.06	1.09	8.29	190.29	5.86	0.98
Brine 4	0.38	39.80	15.40	1.55	173.00	0.38	0.23	ND	230.70	7.27	0.93
Brine 23	0.47	15.50	10.20	1.05	83.00	0.25	0.19	ND	110.70	3.27	0.98
Basque Lake #4											
Brine 1	0.48	49.00	27.30	0.69	221.00	0.00	1.27	7.62	299.70	9.27	0.98
Salt Lake											
Brine 1	0.13	14.80	8.86	0.72	73.40	0.22	0.98	8.11	98.13	2.97	0.99
Last Chance Lake											
Brine 1	0.00	0.05	53.60	5.71	18.90	82.30	12.40	ND	160.56	4.49	ND
Brine 4	0.00	0.02	51.20	4.15	13.50	78.40	12.40	9.99	159.70	4.17	0.96
Brine 5	0.01	0.07	82.10	6.97	22.90	62.80	17.60	9.89	192.40	4.60	0.93

Note. Concentrations of ions are reported in g/L. Salinity is reported in parts per thousand (ppt). ND values represent lakes for which measurements were not determined.

On average, Basque Lake #1 had the highest TOC (mean 16.63%) and Salt Lake the lowest (mean 0.79%) with Basque Lake #2, Basque Lake #4, and Last Chance Lake falling intermediate. Microbial mats and sediments had higher TOC than salts and brines with the exception of salt dissolution residues from Basque Lake #1 and brines from Last Chance Lake. The average ratio between TOC in the sediment ($TOC_{sediment}$) relative to POM in the brine (POM_{brine}) is used to normalize the sedimentary accumulation of OM to that produced in the water column between lakes. These calculations showed that Mg-SO_4 dominated lakes had high $TOC_{sediment}/POM_{brine}$ ratios (average 20.7) compared to the Na-CO_3 lake (average 2.8). The carbon isotopic composition of bulk OM varied considerably between lakes with the most ^{13}C-enriched values deriving from Basque Lake #1 (mean −16.6‰) and the most ^{13}C-depleted from Last Chance Lake (mean −24.8‰) (Figure 3d). These values also

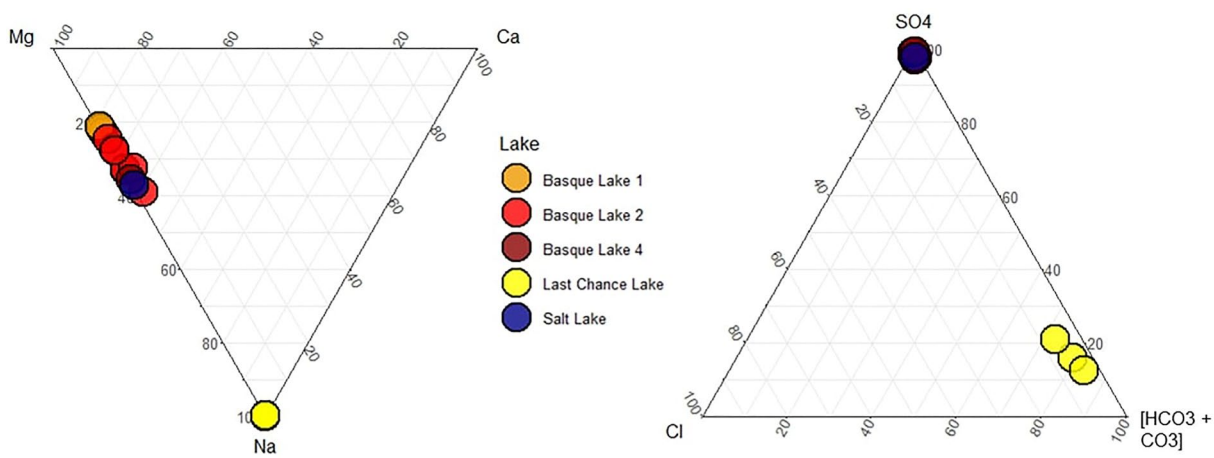

Figure 2. Major ion geochemistry of lake water. Ternary diagrams of the molar fraction of the major cations (left) and major anions (right).

Table 2
Measured Values for Bulk Organic Matter

Season	Brine pool	Type	TLE	TOC (%)	TLE/TOC	$\delta^{13}C$ (VPDB)	$\delta^{15}N$ (AIR)	TN (%)
Basque Lake #1								
Summer	BL1-1	Mat	7.80	12.26	0.64	−12.74	BDL	BDL
Summer	BL1-1	Salt	0.57	42.75	0.01	−16.57	BDL	BDL
Summer	BL1-1	Sediment	6.67	8.75	0.76	−18.12	BDL	BDL
Summer	BL1-2	Brine	2.61	0.46	5.70	−22.21	BDL	BDL
Summer	BL1-2	Mat	7.02	16.54	0.44	−16.88	BDL	BDL
Basque Lake #2								
Winter	BL2	Brine	2.08	0.13	15.42	−21.01	6.95	0.01
Winter	BL2	Ice	3.86	0.15	25.86	−21.96	7.29	0.02
Winter	BL2	Salt	1.01	0.27	7.87	−16.73	8.65	0.03
Winter	BL2	Sediment	6.25	1.23	9.33	−18.19	9.36	0.12
Summer	BL2-1	Brine	2.54	0.97	2.62	−17.78	BDL	BDL
Summer	BL2-1	Sediment	7.91	1.66	7.28	−18.75	8.54	0.17
Summer	BL2-11	Mat	15.70	BDL	BDL	BDL	BDL	BDL
Summer	BL2-2	Brine	1.30	0.86	1.51	−15.11	BDL	BDL
Summer	BL2-23	Brine	1.95	0.85	2.28	−17.57	BDL	BDL
Summer	BL2-23	Mat	10.28	23.08	0.45	−15.09	BDL	BDL
Summer	BL2-23	Salt	2.71	BDL	BDL	BDL	BDL	BDL
Summer	BL2-23	Sediment	6.40	12.53	0.51	−13.12	BDL	BDL
Summer	BL2-3	Brine	4.81	BDL	BDL	BDL	BDL	BDL
Summer	BL2-3	Salt	0.38	BDL	BDL	BDL	BDL	BDL
Summer	BL2-3	Sediment	6.51	0.67	31.70	−16.15	7.72	0.06
Summer	BL2-4	Brine	3.13	1.03	3.03	−19.79	BDL	BDL
Summer	BL2-41b	Sediment	6.29	BDL	BDL	BDL	BDL	BDL
Summer	BL2-44b	Mat	3.34	BDL	BDL	BDL	BDL	BDL
Basque Lake #4								
Summer	BL4	Brine	1.10	0.31	3.53	−20.32	BDL	BDL
Summer	BL4	Salt	0.28	BDL	BDL	BDL	BDL	BDL
Summer	BL4	Sediment	5.91	9.68	0.61	−17.52	BDL	BDL
Last Chance Lake								
Winter	LCL1	Brine	0.55	0.05	10.41	−28.30	5.05	0.01
Winter	LCL1	Ice	5.32	0.08	55.03	−27.64	6.34	0.01
Winter	LCL1	Salt	0.24	0.30	0.60	−22.84	5.14	0.00
Summer	LCL1	Sediment	2.95	0.78	5.13	−24.76	10.73	0.05
Summer	LCL1	Mat	5.23	2.27	40.72	−23.22	12.18	0.22
Summer	LCL4	Brine	1.03	0.78	1.33	−25.24	BDL	BDL
Summer	LCL4	Mat	8.47	2.63	3.22	−26.44	BDL	BDL
Summer	LCL4	Sediment	1.34	1.39	0.97	−24.27	BDL	BDL
Summer	LCL5	Brine	1.07	0.28	3.77	−25.70	BDL	BDL
Summer	LCL5	Mat	3.17	0.95	3.34	−25.51	BDL	BDL
Summer	LCL5	Sediment	1.59	0.92	1.72	−24.27	BDL	BDL
Salt Lake								

Table 2
Continued

Season	Brine pool	Type	TLE	TOC (%)	TLE/TOC	$\delta^{13}C$ (VPDB)	$\delta^{15}N$ (AIR)	TN (%)
Winter	SL	Brine	0.78	0.06	18.80	−24.57	3.07	0.01
Winter	SL	Ice	2.57	0.09	28.20	−28.34	6.90	0.00
Winter	SL	Salt	0.45	0.14	4.40	−23.91	7.47	0.01
Winter	SL	Sediment	8.07	0.49	19.14	−21.78	6.60	0.06
Summer	SL1	Brine	3.16	BDL	BDL	BDL	BDL	BDL
Summer	SL1	Salt	0.21	0.02	6.82	−20.79	9.89	0.00
Summer	SL1	Sediment	3.34	2.52	1.66	−21.25	9.05	0.29

Note. Total Lipid Extract (TLE), Total Organic Carbon (TOC), Total Nitrogen (TN) and carbon/nitrogen stable isotope compositions. BDL (below detection limit) values represent lakes for which samples measurements could not be determined due to sample material limitations.

varied by sample type with the most ^{13}C-enriched values deriving from the sediments and most ^{13}C-depleted from the POM.

The concentration of total nitrogen (TN) and its isotopic composition varied within and between lakes (Figure 3b) but was often at or below the level of detection with our methods. Samples from Basque Lake #2, Last Chance Lake, and Salt Lake had TN values that spanned a relatively large range from below the limit of detection to 0.3% N. Samples from Basque Lake #1 and #4 yielded low TON, typically below analytical limits. The isotopic composition of nitrogen ($\delta^{15}N_{TN}$), where measurable, also varied widely between and within lakes exhibiting more ^{15}N-enriched average values in samples from Last Chance Lake, intermediate values in those from the Basque lakes, and more ^{15}N-depleted values in those from Salt Lake (Figure 3e).

The total lipid extracts (TLE) showed similar mean values between lakes but large distributions (Figure 3c). Mean TLE concentrations ranged from 2.42 to 5.11 mg per gram of sediment and varies systematically by sample type. Generally, the sediments and microbial mats have the highest TLE in all lakes except Last Chance Lake where POM (in mg/L filtered) is the highest. Conversely, the salt samples consistently had the lowest concentrations of TLE in all lakes. The TLE concentrations for brines typically fell between sediments and salts.

To estimate the production of lipids with respect to OM, we calculated the relative proportion of total lipids relative to OM (TLE/TOC) for each sample (Figure 3f). The highest mean ratios of TLE/TOC are found in salts with the exception of Salt Lake and Basque Lake #4. Additionally, within individual lakes, brines generally have a higher TLE/TOC ratio (representing a higher relative lipid contribution) than sediments except for Basque Lake #2 which shows a higher proportion of TLE/TOC in the sediments relative to the brines. Including all sample types, Basque Lake #1 recorded the highest ratios of TLE/TOC (14.12) whereas Basque Lake #4 recorded the lowest average ratio (2.07).

4.3. Lipid Composition and Distribution

We detected a variety of lipid compounds in all sample types including fatty acids, alkanes, and ether-bound lipids (Figure 4). Fatty acids were more abundant than alkanes in the ester-bound fractions. Alkanes were measured but are minor contributors (<5%) to the lipid distribution in the mat, POM, and salt samples, although they do comprise a moderate proportion (~10%-20%) in sediment samples. Similarly, ether-bound lipids constitute a very minor proportion (<1%) of the total lipids recovered from these samples, although this may be due to a known problem of low yields of this method (Kaneko et al., 2011).

Sediments and mat samples contained the greatest diversity of fatty acids, with 54 unique compounds present. The distribution of fatty acids is broadly similar across sample types and sites. POM samples consistently contained primarily short saturated and monounsaturated fatty acids (MUFAs). Sediment samples show the greatest diversity of fatty acids across sites and include an abundance of long saturated and branched fatty acids. The sediments also show a decrease in the proportion of MUFAs relative to short saturated compounds. The most abundant fatty acids in our samples were *n*-$C_{16:0}$, $C_{16:1}$, $C_{16:2}$, *n*-$C_{18:0}$, and $C_{18:1}$; however, the carbon chain lengths

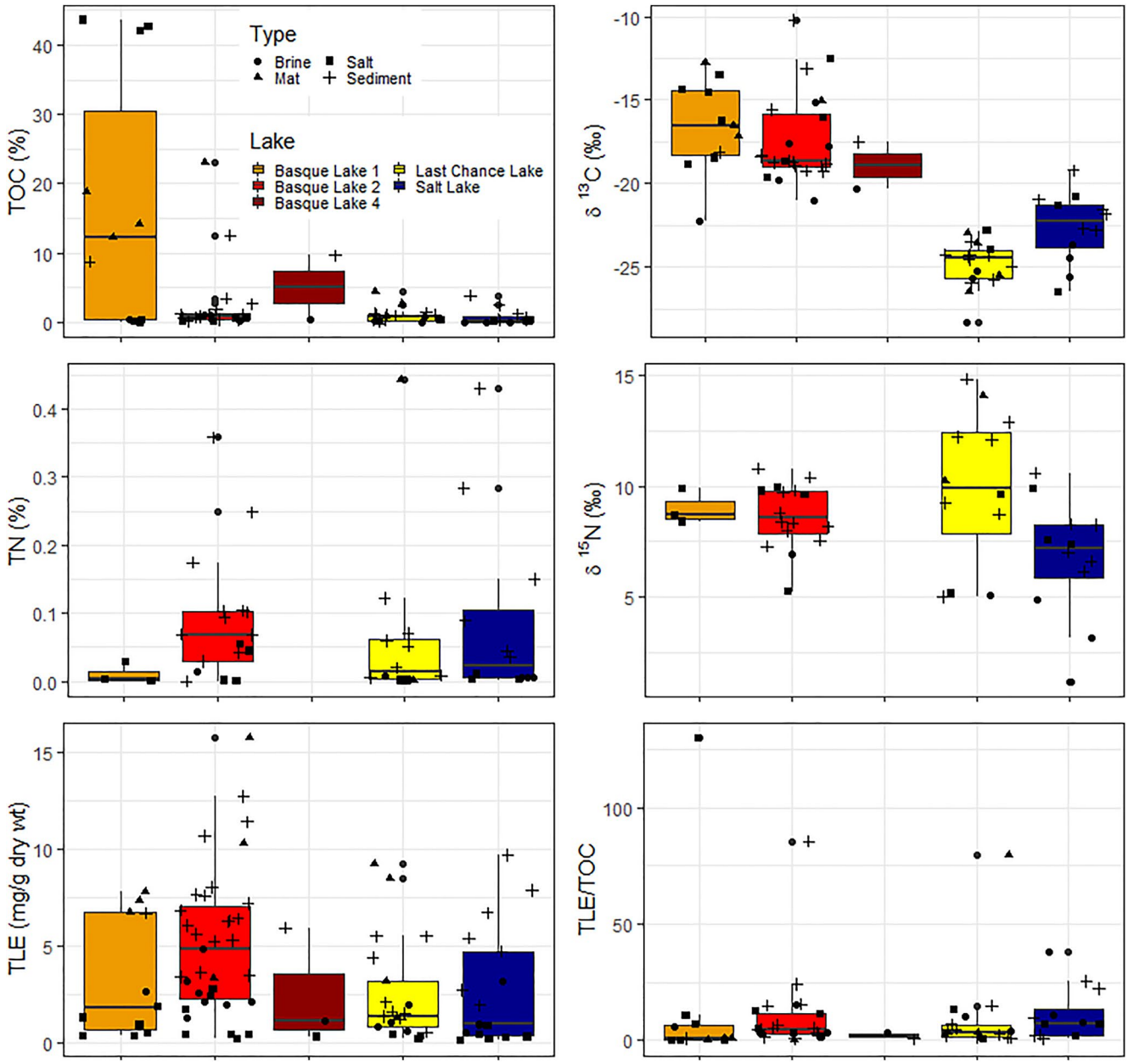

Figure 3. Box and whisker plot of bulk organic matter parameters. (a) Total Organic Carbon Abundance, (b) Total Nitrogen Abundance, (c) Total Lipid Extract, (d) $\delta^{13}C$ Isotopic Composition of Organic Matter, (e) $\delta^{15}N$ Isotopic Composition of Samples, (f) Lipid Production as mg of TLE with respect to g of Organic Carbon.

present ranged from C_{12} to C_{32}. The *i*-$C_{14:0}$, *i*-$C_{15:0}$, *a*-$C_{15:0}$, and *a*-$C_{16:0}$, and *i*-$C_{17:0}$ branched fatty acids are also present in many samples with *i*-$C_{15:0}$ and *a*-$C_{15:0}$ being the most abundant. The *i*-$C_{17:0}$, *a*-$C_{16:0}$ and *i*-$C_{14:0}$ are relatively abundant. Across all sample types, there is an even-over-odd preference in the fatty acid distribution. This is especially apparent in the POM and mat samples where there was a strong even-chain fatty acid presence above carbon chain length 18. The long chain saturated fatty acids from the sediments also show this pattern although odd-chain fatty acids are present. We identified both isoprenoidal and non-isoprenoidal products from cleavage of ether-bound lipids. The primary isoprenoidal ether-bound lipid identified was phytane (*iso*-C20) whereas the primary non-isoprenoidal product was *n*-$C_{16:0}$ and *n*-$C_{18:0}$. Ether-bound lipids, including both isoprenoidal and non-isoprenoidal, were most abundant in Last Chance Lake.

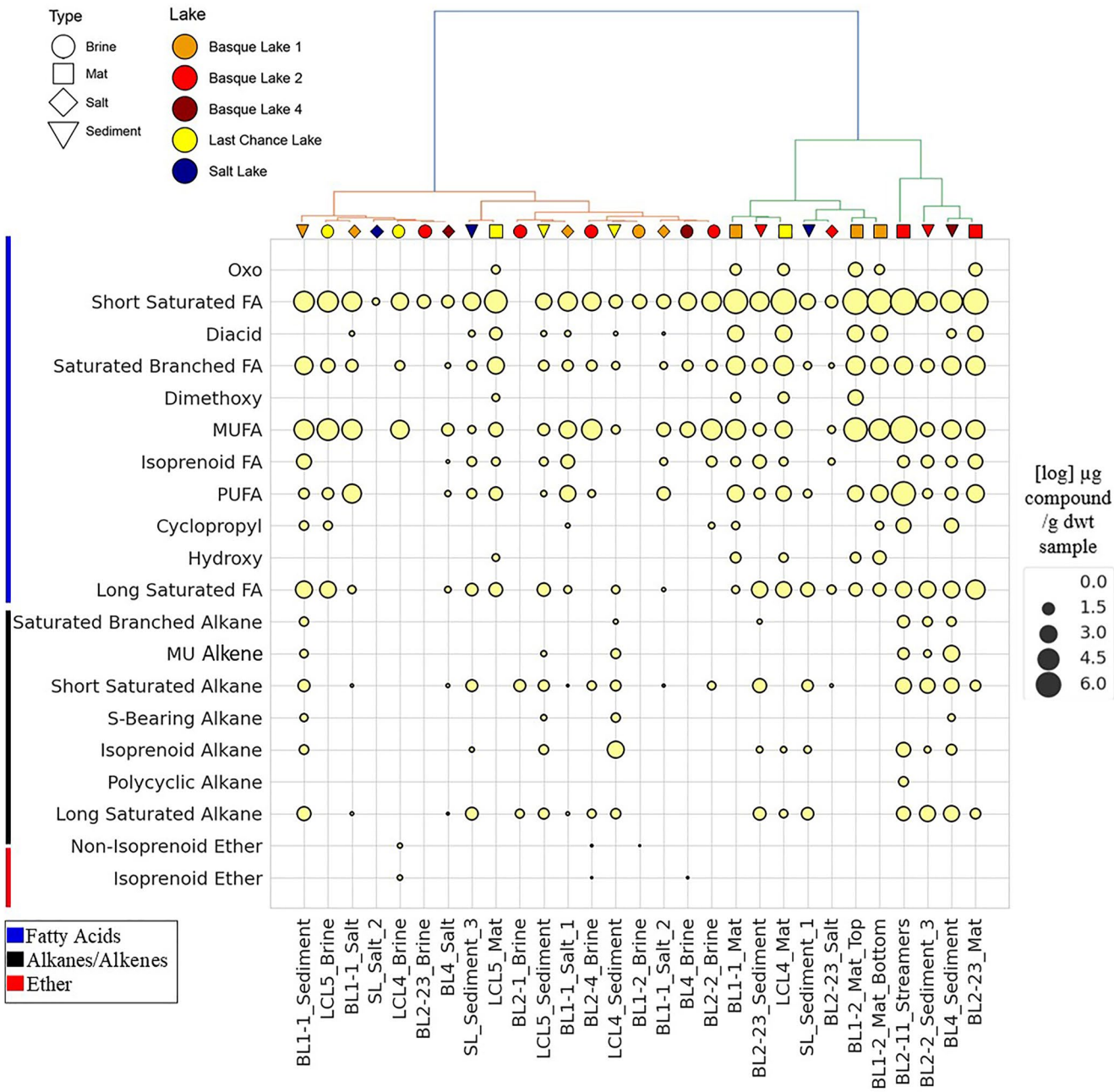

Figure 4. Lipid composition and abundance. Summed concentrations of lipid classes are represented with respect to samples. Bubble size represents $\log_2$ concentrations of µg compound/g sample dry weight (dwt). Samples are arranged based on hierarchical clustering using Ward's method. The orange and green colors of the dendrogram represent the two distinct clusters within our samples. The blue bar indicates fatty acids, the black bar indicates alkanes, and the red bar indicates ether-bound lipids.

5. Discussion

5.1. Lipid Biomarker Production

Lipid biomarkers are semi-quantitative and markers of taxonomy when extracted with consistent methods and referenced to internal standards. Membrane-derived lipid biomarkers are often taxonomically resolved to the domain, and sometimes finer levels, which allows for a differentiation of lipid sources (Brocks & Pearson, 2005; Pearson, 2014; Peters, 2005). Bacteria typically contain membranes composed of diacyl glycerides where fatty acids are ester-linked to glycerol backbones with a range of polar head groups (Willers et al., 2015). In these

membranes fatty acid moieties are typically 14–22 carbons long, including mono- and dialkenes, and branches, or cyclopropyl rings (Sohlenkamp & Geiger, 2016; Willers et al., 2015). While less typical, some bacteria are also able to synthesize ether-bound lipids with alkyl chains usually 15 or 16 carbons long (Bale et al., 2021; Grossi et al., 2015). Terrestrial plants produce leaf waxes composed of fatty acids and *n*-alkanes generally dominated by carbon chain lengths ranging from 25 to 31 (Bush & McInerney, 2013; Diefendorf et al., 2011). Archaea synthesize ether-linked isoprenoidal lipid membranes with either diethers, tetraethers, or a combination and can feature a variety of rings and hydroxyl group modifications (Schouten et al., 2013).

Different lipid classes also show varying reactivities toward microbially mediated processes and therefore certain classes have a potential for long term preservation. However, the relative lability of lipids is also dependent on local depositional conditions, including temperature, oxidation state, and importantly, salinity (Canuel & Martens, 1996; Harvey et al., 1986; Middleburg, 1989; Schouten et al., 2010; Sun et al., 1997). For instance, studies have shown that under oxic conditions, lipids degrade more quickly than under otherwise similar anoxic ones (Canuel & Martens, 1996; Sun et al., 1997). Fatty acids are generally more labile than alkanes, thus, in sedimentary systems they can represent either an active microbial community or well-preserved OM. Conversely, alkanes are more refractory and often by-products of degradation reactions or plant material, ultimately, recording a terrestrial or past community. Ether-linkages in lipids are very stable and thus ether lipids are generally well preserved in the geologic record (Schouten et al., 2013).

The lipid biosignature profiles found in the BC lakes across all sample types suggest that microbial biomass produced within the lakes (indicated by short chain, saturated and unsaturated fatty acids), rather than plant-based allochthonous material (long chain alkanes and fatty acids) is the dominant source of OM in these systems, despite the heavily vegetated watersheds. This conclusion is supported by relative dominance of monounsaturated lipids (>50% relative abundance) in POM and sediments (Willers et al., 2015). Surface sediments show elevated concentrations of long saturated fatty acids (>5% relative abundance) and long chain *n*-alkanes with respect to the POM (<5% relative abundance), showing the incorporation of material from surrounding vegetation into sediment; however, the dominant biosignature remains microbial. Further, branched fatty acids, which are generally attributed to a bacterial source, are found in elevated concentrations in microbial mat and sediment samples. While other work has shown short and medium length terminally-branched fatty acids can also be produced by other organisms such as plants, those molecules have only been documented up to a carbon chain length of 12, shorter than those we observe (Kroumova et al., 1994). The presence of the terminally branched fatty acids *i*-C_{15}, *a*-C_{15}, and *i*-C_{17} in the hypersaline lakes is often attributed to the presence of gram-positive and sulfate reducing bacteria (SRB; Tan et al., 2018; Vestal & White, 1989; O'Leary & Wilkinson, 1988; Perry et al., 1979). Given the fatty acid chain lengths, high concentrations of SO_4^{2-} in our lakes, the presence of elemental sulfur, and sulfide within the sediments, an SRB origin is reasonable. The increased abundance of branched fatty acids in sediments compared to POM, specifically *a*-C_{15} further suggests the role of SRB as these anaerobes will increase in abundance in anoxic settings (Tan et al., 2018). Moreover, the presence and abundance of the MUFAs $C_{16:1}$ and $C_{18:1}$ within the brines is consistent with the lipids generally produced by cyanobacteria, algae, as well as many gram-negative bacteria (Ahlgren et al., 1992; Willers et al., 2015; Zelles et al., 1997). Plants may also produce such MUFAs (Kazaz et al., 2022); however, plants will generally have a higher atomic C/N ratio than aquatic organisms (Meyers, 1994; see Section 5.3 below).

The dominance of short-chain as opposed to long-chain fatty acids and alkane biomarkers indicates that an extant microbial community is producing lipids that are being incorporated into the shallow sediments. This distribution is in contrast to that found at other Martian analog systems such as the acidic SO_4-rich hypersaline lakes in Western Australia which show a greater proportion of alkanes and long-chain fatty acids (Johnson et al., 2020), and are attributed primarily to inputs from allochthonous vegetation. Further, in the Basque Lakes we find that ether-bound lipids are in low abundance relative to ester-bound lipids and include isoprenoidal (archeal-derived) and non-isoprenoidal (bacterial-derived), which suggests a dominantly bacterial rather than archeal biomarker signature. Our observation of minor archeal lipid inputs is consistent with the metagenomic analysis presented by Pontefract et al. (2017) of a nearby SO_4-rich hypersaline lake which found only minor contributions of archaea to the microbial community. The low concentrations of Na^+ in our study sites may be responsible for the minor archeal lipid inputs as studies have shown that halophilic archaea require a minimum NaCl concentration of 1.5 M for optimum cell growth (Bowers & Wiegel, 2011; Mesbah & Wiegel, 2008; Robinson et al., 2005). Additionally, many halophilic archaea require a minimum pH of 8.5 (Bowers & Wiegel, 2011). These bounds are consistent with our results as the only lake with elevated archeal lipid concentrations was the alkaline Na-CO_3 dominated lake.

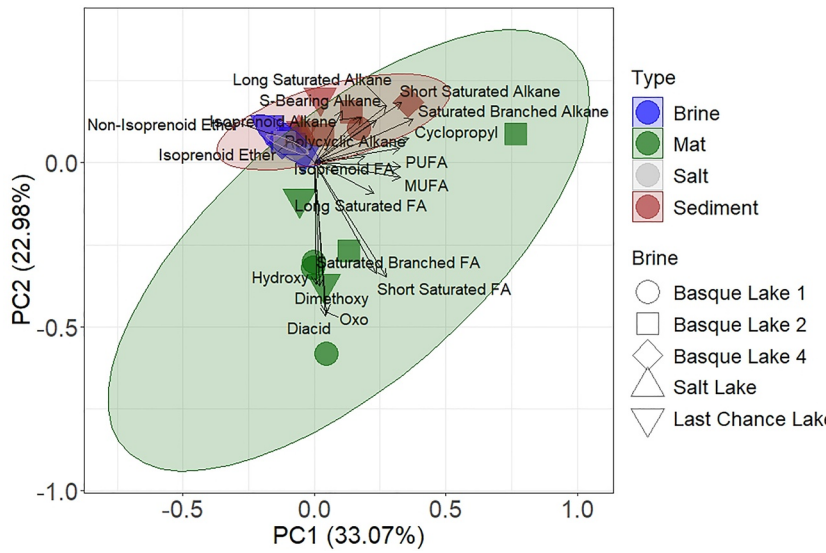

Figure 5. A principal component analysis (PCA) of our samples. Vectors were computed for compounds that contributed variance on the samples. Ellipses represent 95% confidence intervals for each sample type.

5.2. Sample Variation of Lipid Composition

A key motivating question of this study is how kosmotropic and chaotropic ions affect biosignature production and how this varies across chemical gradients within hypersaline systems. To reduce the inherent complexity in environmental samples and their chemical compositions, we performed a principal component analysis (PCA). This analysis allows us to discern which lipid biomarkers control the variation across and between samples. While the lakes varied spatially and chemically, the PCA analysis shows that the lipid distribution is most influenced by sample type (Figure 5). Brine and salt samples were most similar to each other in this ordination, and sediment and mat samples also trended together. The link between brines and salts could suggest that microbes aid in the formation and precipitation of salts (saturated or unsaturated solutions) either by providing a nucleation site or by promoting precipitation through metabolic activities (Cabestrero et al., 2018; Cangemi et al., 2016). Alternatively, material from the brine could be simply trapped within precipitating salts (Cabestrero et al., 2018). The sampled microbial mats were benthic, likely incorporating some surface sediments, which explains the similarity in lipid composition between these and sediment samples. Additionally, the abundance of alkanes differentiates the sediment samples from all other sample types as shown by the computed eigenvectors. In contrast, brines are differentiated by their presence, albeit low concentrations, of ether-bound lipids (Figure 5). Considering the PCA shows a relatively strong clustering by sample type rather than chemical composition (i.e., kosmotropic $MgSO_4$ solutions vs. chaotropic Na_2CO_3 solutions) of the lakes, this might suggest that the primary mechanism controlling the lipid distributions in these lakes are factors not included in this study such as sediment morphology, sedimentation rate, or mean annual temperature.

5.3. Bulk Organic Matter Abundances and Isotopic Values

Bulk organic parameters such as TOC, TN, and $\delta^{13}C_{TOC}$ values integrate both biomass production and degree of degradation (Meyers, 2003) and can be used to constrain the sources of biomass in lacustrine systems (i.e., land-derived or aquatic-derived; Meyers, 2003; Meyers, 1994). For instance, OM from algae tends to be protein-rich producing a C/N ratio between four and ten (Meyers, 1994, 2003), whereas vascular plant biomass is protein-poor but cellulose rich, producing high C/N ratios reaching values of 20 or greater (Meyers, 1994, 2003). $\delta^{13}C_{TOC}$ values provide complementary information reflecting the mechanisms of carbon fixation and assimilation (Hayes, 2001; Meyers, 2003).

Bulk organic measurements described here provide further evidence that the primary biosignature is of in situ microbial origin rather than exogenous material (Figure 6). Data from the SO_4-dominated lakes (Basque Lake and

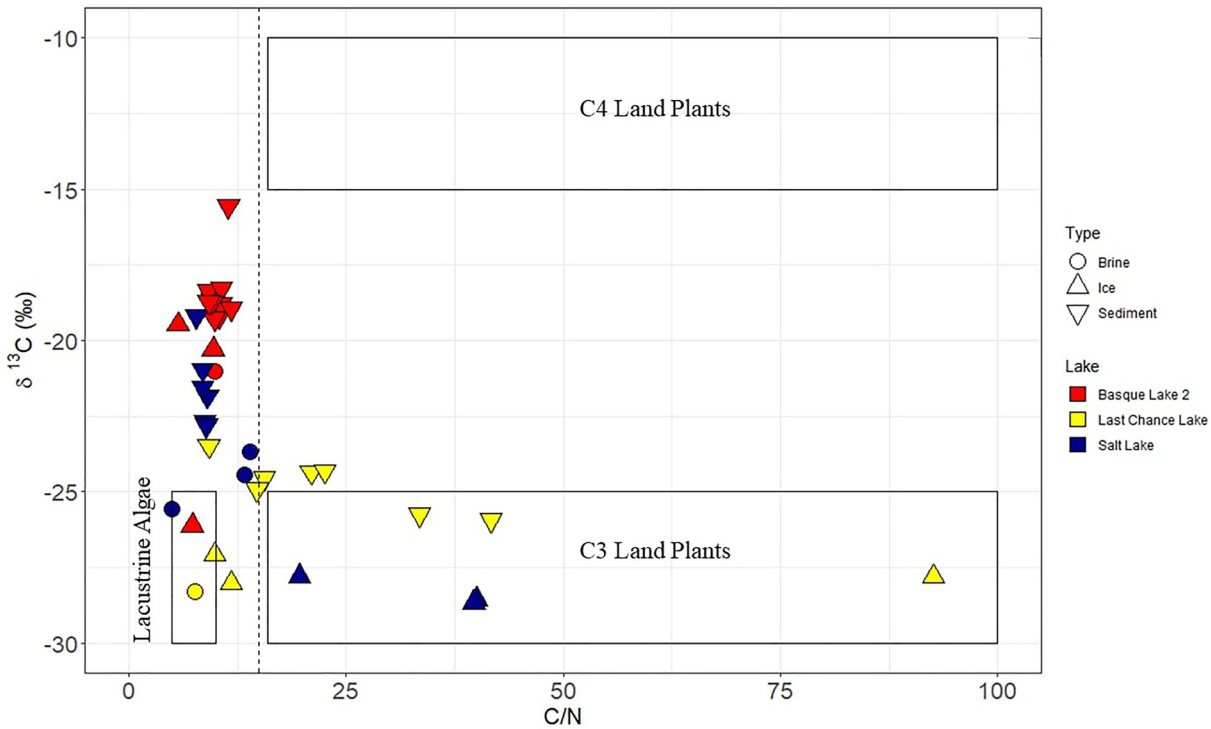

Figure 6. Cross-plot showing the relationship between C/N ratio and bulk carbon isotopic composition of OM from sediments and water. The dashed line indicates the typical cutoff for an aquatic versus terrestrial signature of 15 (Meyers, 1994) and boxes represent the general composition for lacustrine algae and C_4 and C_3 land plants.

Salt Lake) group together with low C/N and ^{13}C-enriched isotope values consistent with an increase in microbial productivity (Meyers, 2003). In contrast, the CO_3-dominated lake, Last Chance Lake, shows ^{13}C-depleted OM that ranges to very high C/N values. This overall pattern of ^{13}C-depleted OM and high C/N values suggests a mixed OM signal resulting from either exogenous input or a higher degree of degradation (Meyers, 1994).

To differentiate between production potential and degree of degradation, we calculated $TOC_{sediment}/POM_{brine}$ ratios. The Mg-SO_4 lakes have the highest values with respect to the CO_3-dominated lake, suggesting a slower rate of organic carbon remineralization within the Mg-SO_4 lakes, ultimately, leading to an increase in the concentration of TOC in the sediment with respect to what is produced in the brine. These results agree with the bulk isotope data. Alternatively, this higher ratio could be driven in part by a productive anaerobic community in the surface sediments. Elevated concentrations of the branched fatty acids *i*-C_{15}, *a*-C_{15}, and *i*-C_{17} in the sediments of these lakes support this mechanism.

5.4. Sulfate-Rich Lakes

As Mars transitioned from a wet to dry climate, an abundance of Cl and SO_4-rich deposits were formed (Pontefract et al., 2017; Tosca et al., 2008). As such, due to the abundance of Cl systems on Earth, many hypersaline environments investigated as Mars analogs are Cl-dominated. These sites such as Don Juan Pond ($CaCl_2$) in Antarctica, the Discovery Basin ($MgCl_2$) in the Mediterranean, and the South Bay Salt Work Bitterns (NaCl and $MgCl_2$ gradient) in Southern California are some of the lowest biomass places on Earth, with both low microbial diversity and preservation of organic material (Dickson et al., 2013; Hallsworth et al., 2007; Klempay et al., 2021). This begs the question, what is the production and preservation potential of lipid biomarkers in other aqueous solutions of varying kosmotropic or membrane stabilizing settings?

Extremely SO_4-rich aqueous environments are rare on Earth but are known from geographic regions like South-Central British Columbia and Western Australia (Johnson et al., 2020; Pontefract et al., 2017). Previous biosignature work on these Mars-analog environments has shown a range of OM and lipid biomarker production, microbial diversity, or microbial activity. Work done using metagenomic analysis in Spotted Lake (South-Central

British, Columbia), a circumneutral Mg-SO_4 lake, found a diverse and abundant microbial community (Pontefract et al., 2017). In contrast, lipid biosignature analysis in acidic sulfate-rich lakes (Lake Gneiss and Lake Gilmore, Western Australia) showed very low concentrations of microbial lipids, especially short saturated and branched fatty acids (Johnson et al., 2020), which the authors attributed to destruction by the acidic conditions of these Australian lakes. As such, the dominant lipid biosignature observed in the Western Australian lakes were long chain *n*-alkanes and long saturated fatty acids indicating limited microbial biomarker production and a larger terrestrial vegetation input.

The lakes described in our study chemically and physically resemble Spotted Lake and feature similarly abundant microbial biosignatures. These lakes are also potentially representative of ancient Martian brines as they show exceptionally high water activities and high ionic strengths similar to those simulated on ancient Martian surface (Fox-Powell et al., 2016). Yet, despite these ionic strengths, which is thought to be limiting to life, our data shows an abundance of microbially-derived lipid biomarkers. Our results suggest that these circumneutral Mg-SO_4-dominated hypersaline environments feature high OM production and abundant microbial life. This corroborates the metagenomic work done by Pontefract et al., 2017 in Spotted Lake, and is in significant contrast to the Western Australian lakes studied by Johnson et al., 2020 and other Mars analog environments such as Cl-dominated hypersaline systems which have shown limited microbial life via 16s rRNA sequencing, low abundance biosignatures and poor preservation of lipid, and limited microbial activity (Dickson et al., 2013; Hallsworth et al., 2007; Johnson et al., 2020; Klempay et al., 2021). The implication of this difference suggests that circumneutral Mg-SO_4 dominated hypersaline systems have greater biosignature production potential. Ultimately, this chemical composition may be a better target for astrobiological investigation than their acidic or Cl-dominated counterparts.

6. Conclusions

We find abundant OM production with biosignatures consistent with microbial origin within the hypersaline SO_4-dominated lakes of the Cariboo Plateau. These signatures are typical of compounds produced by microbes, specifically sulfate reducing bacteria, gram-positive bacteria, and cyanobacteria, rather than material derived from surrounding vegetation or archaea. We do observe an increase in lipid diversity, including terrestrially derived material, in sediments indicating incorporation of externally produced lipids into the sediments. The refractory lipids are likely present in the brines below detection limit. However, they ultimately get concentrated in the sediments due to a lack of remineralization in the brines. Additionally, labile lipids detected in the surface sediments likely reflect a combination of sedimented POM, biomass produced by benthic mats and bacteria within the sediments, and the surrounding landscape. Comparison between lakes targeted here suggests that kosmotropic Mg-SO_4 dominated environments show greater OM abundance and microbial lipid biosignatures than those of other chemistries, specifically chaotropic Cl environments.

Overall, our study highlights that despite their extreme salinities and ionic strengths, these saturated Mg-SO_4 brines of circumneutral to alkaline pH are teeming with life, producing an abundance of lipid biosignatures. Additionally, despite the Mg^{2+} cation being highly chaotropic, the presence of the compensating kosmotropic anion SO_4^{2-} appears to negate the destabilizing effects of the Mg^{2+} ion as observed by the abundance of microbial lipid biomarkers. These lipid profiles are distinct from those found in Cl-dominated environments as bacteria are the dominant lipid-producing microorganisms rather than archaea and algae. Compared to other terrestrial Mars-analog environments these systems show excellent production potential for organics, which is directly informative for current and future life-detection missions. While we have demonstrated the production of lipid biosignatures in the shallowest sediments, future work will target how well these biosignatures are preserved on geologic timescales.

Data Availability Statement

All data, R, and Python scripts written for data analysis and visualization are hosted at https://zenodo.org/record/8169323 and can be cited as "F. Nichols (2023).

Acknowledgments
This work was supported by a grant from NASA Exobiology to AP and MRO (NNH17ZDA001N-EXO). Drone images were taken by Mitchell Barklage, PhD. MRO is a fellow in the CIFAR Earth 4D program. This work would not have been possible without the aid in sample/data collection from Christopher Carr, PhD; Jacob Buffo, PhD; and Emma Brown (Georgia Tech University). We are also very grateful to both reviewers who provided constructive edits and improved the manuscript significantly.

References

Ahlgren, G., Gustafsson, I.-B., & Boberg, M. (1992). Fatty Acid content and chemical composition of freshwater microalgae. *Journal of Phycology*, *28*(1), 37–50. https://doi.org/10.1111/j.0022-3646.1992.00037.x

Aubrey, A., Cleaves, H. J., Chalmers, J. H., Skelley, A. M., Mathies, R. A., Grunthaner, F. J., et al. (2006). Sulfate minerals and organic compounds on Mars. *Geology*, *34*(5), 357–360. https://doi.org/10.1130/g22316.1

Bale, N. J., Ding, S., Hopmans, E. C., Arts, M. G. I., Villanueva, L., Boschman, C., et al. (2021). Lipidomics of environmental microbial communities. I: Visualization of component distributions using untargeted analysis of high-resolution mass spectrometry data. *Frontiers in Microbiology*, *12*. https://doi.org/10.3389/fmicb.2021.659302

Benison, K. C., & Karmanocky, F. J., III. (2014). Could microorganisms be preserved in Mars gypsum? Insights from terrestrial examples. *Geology*, *42*(7), 615–618. https://doi.org/10.1130/g35542.1

Bligh, E. G., & Dyer, W. J. (1959). A rapid method of total lipid extraction and purification. *Canadian Journal of Biochemistry and Physiology*, *37*(8), 911–917. https://doi.org/10.1139/y59-099

Bowers, K. J., & Wiegel, J. (2011). Temperature and pH optima of extremely halophilic archaea: A mini-review. *Extremophiles*, *15*(2), 119–128. https://doi.org/10.1007/s00792-010-0347-y

Brocks, J. J., & Pearson, A. (2005). Building the biomarker tree of life. *Reviews in Mineralogy and Geochemistry*, *59*(1), 233–258. https://doi.org/10.2138/rmg.2005.59.10

Bush, R. T., & McInerney, F. A. (2013). Leaf wax n-Alkane distributions in and across modern plants: Implications for paleoecology and chemotaxonomy. *Geochimica et Cosmochimica Acta*, *117*(15), 161–169. https://doi.org/10.1016/j.gca.2013.04.016

Cabestrero, O., del Buey, P., & Sanz-Montero, M. E. (2018). Biosedimentary and geochemical constraints on the precipitation of mineral crusts in shallow sulphate lakes. *Sedimenary Geology*, *366*, 32–46. https://doi.org/10.1016/j.sedgeo.2018.01.005

Cangemi, M., Censi, P., Reimer, A., D'Alessandro, W., Hause-Reitner, D., Madonia, P., et al. (2016). Carbonate precipitation in the Alkaline lake Specchio di Venere (Pantelleria Island, Italy) and the possible role of microbial mats. *Applied Geochemistry*, *67*, 168–176. https://doi.org/10.1016/j.apgeochem.2016.02.012

Canuel, E. A., & Martens, C. S. (1996). Reactivity of recently deposited organic matter: Degradation of lipid compounds near the sediment-water interface. *Geochemica and Cosmochemica Acta*, *60*(10), 1793–1806. https://doi.org/10.1016/0016-7037(96)00045-2

Carrizo, D., Sánchez-García, L., Rodriguez, N., & Gómez, F. (2019). Lipid biomarker and carbon stable isotope survey on the dallol hydrothermal system in Ethiopia. *Astrobiology*, *19*(12), 1474–1489. https://doi.org/10.1089/ast.2018.1963

Cheng, Z., Xiao, L., Wang, H., Yang, H., Li, J., Huang, T., et al. (2017). Bacterial and archaeal lipids recovered from subsurface evaporites of dalangtan playa on the Tibetan plateau and their astrobiological implications. *Astrobiology*, *17*(11), 1112–1122. https://doi.org/10.1089/ast.2016.1526

Collins, K. D. (1997). Charge density-dependent strength of hydration and biological structure. *Biophysical Journal*, *72*(1), 65–76. https://doi.org/10.1016/s0006-3495(97)78647-8

Cui, Y., Miller, D., Schiarizza, P., & Diakow, L. J. (2017). British Columbia digital geology. *British Columbia ministry of energy, mines and petroleum resources, British Columbia geological survey open file 2017-8* (p. 9). Data version 2019-12-19.

Dickson, J. L., Head, J. W., Levy, J. S., & Marchant, D. R. (2013). Don Juan Pond, Antarctica: Near-surface CaCl(2)-brine feeding Earth's most saline Lake and implications for Mars. *Scientific Reports*, *3*(1), 1166. https://doi.org/10.1038/srep01166

Diefendorf, A. F., Freeman, K. H., Wing, S. L., & Graham, H. V. (2011). Production of n-Alkyl lipids in living plants and implications for the geologic past. *Geochimica et Cosmochimica Acta*, *75*(23), 7472–7485. https://doi.org/10.1016/j.gca.2011.09.028

Ehlmann, B. L., Mustard, J. F., Murchie, S. L., Poulet, F., Bishop, J. L., Brown, A. J., et al. (2008). Orbital identification of carbonate-bearing rocks on Mars. *Science*, *322*(5909), 1828–1832. https://doi.org/10.1126/science.1164759

Fisher, L. A., Pontefract, A., M. Som, S., Carr, C. E., Klempay, B., E. Schmidt, B., et al. (2021). Current state of athalassohaline deep-sea hypersaline anoxic basin research – Recommendations for future work and relevance to astrobiology. *Environmental Microbiology*, *23*(7), 3360–3369. https://doi.org/10.1111/1462-2920.15414

Fox-Powell, M. G., & Cockell, C. S. (2018). Building a geochemical view of microbial salt tolerance: Halophilic adaptation of *Marinococcus* in a Natural magnesium sulfate brine. *Frontiers in Microbiology*, *16*. https://doi.org/10.3389/fmicb.2018.00739

Fox-Powell, M. G., Hallsworth, J. E., Cousins, C. R., & Cockell, C. S. (2016). Ionic strength is a barrier to the habitability of Mars. *Astrobiology*, *16*(6), 427–442. https://doi.org/10.1089/ast.2015.1432

Gattinger, A., Gunthner, A., Schloter, M., & Munch, J. C. (2003). Characterisation of archaea in soils by polar lipid analysis. *Acta Biotechnologica*, *23*(1), 21–28. https://doi.org/10.1002/abio.200390003

Grossi, V., Mollex, D., Vincon-Laugier, A., Hakil, F., Pacton, M., & Cravo-Laureau, C. (2015). Mono- and dialkyl glycerol ether lipids in anaerobic bacteria: Biosynthetic insights from the mesophilic sulfate reducer *Desulfatibacillum alkenivorans* PF2803. *Applied and Environmental Microbiology*, *81*(9), 3157–3168. https://doi.org/10.1128/aem.03794-14

Hallsworth, J. E., Yakimov, M. M., Golyshin, P. N., Gillion, J. L. M., D'Auria, G., de Lima Alves, F., et al. (2007). Limits of life in $MgCl_2$-containing environments: Chaotropicity defines the window. *Environmental Microbiology*, *9*(3), 801–813. https://doi.org/10.1111/j.1462-2920.2006.01212.x

Harvey, H. R., Fallon, R. D., & Patton, J. S. (1986). The effect of organic matter and oxygen on the degradation of bacterial membrane lipids in marine sediments. *Geochimica et Cosmochimica Acta*, *50*(5), 795–804. https://doi.org/10.1016/0016-7037(86)90355-8

Hayes, J. M. (2001). Fractionation of the isotopes of carbon and hydrogen in biosynthetic processes. *Geochimica et Cosmochimica Acta*, *65*.

Hunter, J. D. (2007). Matplotlib: A 2D graphics environment. *Computing in Science & Engineering*, *9*(3), 90–95. https://doi.org/10.1109/mcse.2007.55

Jenkins, O. P. (1918). Spotted lakes of epsomite in Washington and British Columbia. *American Journal of Science*, *46*(275), 638–644. https://doi.org/10.2475/ajs.s4-46.275.638

Johnson, D. B., Beddows, P. A., & Osburn, M. R. (2018). Microbial diversity and biomarker analysis of modern freshwater microbialites from Laguana Bacalar, Mexico. *Geobiology*, *16*(3), 319–337. https://doi.org/10.1111/gbi.12283

Johnson, S. S., Millan, M., Graham, H., Benison, K. C., Williams, A. J., McAdam, A., et al. (2020). Lipid biomarkers in ephemeral acid salt lake mudflat/sandflat sediments: Implications for Mars. *Astrobiology*, *20*(2), 167–178. https://doi.org/10.1089/ast.2017.1812

Kaneko, M., Kitajima, F., & Naraoka, H. (2011). Stable hydrogen isotope measurement of archaeal ether-bound hydrocarbons. *Organic Geochemistry*, *42*(2), 166–172. https://doi.org/10.1016/j.orggeochem.2010.11.002

Kazaz, S., Miray, R., Lepiniec, L., & Baud, S. (2022). Plant monounsaturated fatty acids: Diversity, biosynthesis, functions and uses. *Progress in Lipid Research*, *85*, 101138. https://doi.org/10.1016/j.plipres.2021.101138

Kite, E. S., Gaidos, E., & Onstott, T. C. (2018). Valuing life detection missions. *Astrobiology*, *18*(7), 834–840. https://doi.org/10.1089/ast.2017.1813

Klempay, B., Arandia-Gorostidi, N., Dekas, A. E., Bartlett, D. H., Carr, C. E., Doran, P. T., et al. (2021). Microbial diversity and activity in Southern California salterns and bitterns: Analogues for remnant ocean worlds. *Environmental Microbiology*, *23*(7), 3825–3839. https://doi.org/10.1111/1462-2920.15440

Kroumova, A. B., Xie, Z., & Wagner, G. J. (1994). A pathway for the biosynthesis of straight and branched, odd-and even-length, medium-chain fatty acids in plants. *Proceedings of the National Academy of Sciences*, *91*(24), 11437–11441. https://doi.org/10.1073/pnas.91.24.11437

Mesbah, N. M., & Wiegel, J. (2008). Life at extreme limits the anaerobic halophilic alkalithermophiles. *Annals of the New York Academy of Sciences*, *1125*(1), 44–57. https://doi.org/10.1196/annals.1419.028

Meyers, P. A. (1994). Preservation of elemental and isotopic source identification of sedimentary organic matter. *Chemical Geology*, *114*(3–4), 289–302. https://doi.org/10.1016/0009-2541(94)90059-0

Meyers, P. A. (2003). Applications of organic geochemistry to paleolimnological reconstructions: A summary of examples from the laurentian great lakes. *Organic Geochemistry*, *34*(2), 261–289. https://doi.org/10.1016/s0146-6380(02)00168-7

Middleburg, J. J. (1989). A simple rate model for organic matter decomposition in marine sediments. *Geochimica et Cosmochimica Acta*, *53*(7), 1577–1581. https://doi.org/10.1016/0016-7037(89)90239-1

Nichols, F. (2023). FloydNichols97/BC_Surface_Dataset: Lipid biosignatures in hypersaline lakes. July 20, 2023. Release (version 2.1.0) [Dataset]. Zenodo. https://zenodo.org/record/8169323

Oksanen, J. F., Blanchet, G., Friendly, M., Kindt, R., Legendre, D. M., Minchin, P. R., et al. (2019). vegan: Community ecology package.

O'Leary, W. M., & Wilkinson, S. G. (1988). Gram-positive bacteria. In C. Ratledge & S. G. Wilkinson (Eds.), *Microbial lipids* (pp. 117–185). Academic Press.

Osburn, M. R., LaRowe, D. E., Momper, L. M., & Amend, J. P. (2014). Chemolithotrophy in the continental deep subsurface: Sanford underground research facility (SURF), USA. *Frontiers in Microbiology*, *5*(610). https://doi.org/10.3389/fmicb.2014.00610

Pearson, A. (2014). Lipidomics for geochemistry. In H. D. Holland & K. K. Turekian (Eds.), *Treatise on geochemistry* (2nd ed., Vol. 12, pp. 291–336). Elsevier.

Perry, G. J., Volkman, J. K., Johns, R. B., & Bavor, H. (1979). Fatty acids of bacterial origin in contemporary marine sediments. *Geochimica et Cosmochimica Acta*, *43*(11), 1715–1725. https://doi.org/10.1016/0016-7037(79)90020-6

Peters, K. E. (2005). *The biomarker guide: Biomarkers and isotopes in the environment and Earth history*. Cambridge University Press.

Pontefract, A., Zhu, T., Walker, V. K., Hepburn, H., Lui, C., Zuber, M. T., et al. (2017). Microbial diversity in a hypersaline sulfate lake: A terrestrial Analog of ancient mars. *Frontiers in Microbiology*, *8*, 1819. https://doi.org/10.3389/fmicb.2017.01819

Renaut, R. (1993). Morphology, distribution, and preservation potential of microbial mats in the hydromagnesite-magnesite Playas of the Cariboo Plateau, British Columbia, Canada. *Hydrobiologia*, *267*(1–3), 75–98. https://doi.org/10.1007/bf00018792

Renaut, R., & Long, P. (1989). Sedimentology of the saline lakes of the Cariboo Plateau, Interior British Columbia, Canada. *Sedimentary Geology*, *4*, 239–264. https://doi.org/10.1016/0037-0738(89)90051-1

Renaut, R. W. (1990). Recent carbonate sedimentation and brine evolution in the saline lake basins of the Cariboo Plateau, British Columbia, Canada. In *Saline lakes: Proceedings of the fourth international symposium on Athalassic (inland) saline lakes, held at Banyoles, Spain, May 1988* (pp. 67–81). Springer Netherlands.

Robinson, J. L., Pyzyna, B., Atrasz, R. G., Henderson, C. A., Morrill, K. L., Burd, A. M., et al. (2005). Growth kinetics of extremely halophilic *Archaea* (Family *Halobacteriaceae*) as revealed by Arrhenius plots. *Journal of Bacteriology*, *187*(3), 923–929. https://doi.org/10.1128/jb.187.3.923-929.2005

Schimmelmann, A., Albertino, A., Sauer, P. E., Qi, H., Molinie, R., & Mesnard, F. (2009). Nicotine, acetanilide and urea multi-level ^{2}H-^{13}C- and ^{15}N-abundance reference materials for continuous-flow isotope ratio mass spectrometry. *Rapid Communications in Mass Spectrometry*, *23*(22), 3512–3513. https://doi.org/10.1002/rcm.4277

Schouten, S., Hopmans, E. C., & Sinnighe Damste, J. S. (2013). The organic geochemistry of glycerol dialkyl glycerol tetraether lipids: A review. *Organic Geochemistry*, *54*, 19–61. https://doi.org/10.1016/j.orggeochem.2012.09.006

Schouten, S., Middelburg, J. J., Hopmans, E. C., & Sinninghe Damsté, J. S. (2010). Fossilization and degradation of intact polar lipids in deep subsurface sediments: A theoretical approach. *Geochimica et Cosmochimica Acta*, *74*(13), 3806–3814. https://doi.org/10.1016/j.gca.2010.03.029

Sohlenkamp, C., & Geiger, O. (2016). Bacterial membrane lipids: Diversity in structures and pathways. *FEMS Microbiology Reviews*, *40*(1), 133–159. https://doi.org/10.1093/femsre/fuv008

Sun, M. Y., Wakeham, S. G., & Lee, C. (1997). Rates and mechanisms of fatty acid degradation in oxic and anoxic coastal marine sediments of Long Island Sound, New York, USA. *Geochimica et Cosmochimica Acta*, *61*(2), 341–355. https://doi.org/10.1016/s0016-7037(96)00315-8

Tan, J., Lewis, J. M., & Sephton, M. A. (2018). The fate of lipid biosignatures in a Mars-analogue sulfur stream. *Scientific Reports*, *8*(1), 7586. https://doi.org/10.1038/s41598-018-25752-7

Tosca, N. J., Knoll, A. H., & McLennan, S. M. (2008). Water activity and the challenge for life on Mars. *Science*, *320*(5880), 1204–1207. https://doi.org/10.1126/science.1155432

Vestal, J. R., & White, D. C. (1989). Lipid analysis in microbial ecology. *BioScience*, *39*(8), 535–541. https://doi.org/10.2307/1310976

Wickham, H. (2016). *ggplot2: Elegant graphics for data analysis*. Springer-Verlag.

Wilhelm, M. B., Davia, A. F., Eigenbrode, J. L., Parenteau, M. N., Jahnke, L. L., Liu, X. L., et al. (2017). Xeropreservation of functionalized lipid biomarkers in hyperarid soils in the Atacama Desert. *Organic Geochemistry*, *103*, 97–104. https://doi.org/10.1016/j.orggeochem.2016.10.015

Willers, C., Jansen van Rensburg, P. J., & Claassens, S. (2015). Phospholipid fatty acid profiling of microbial communities–A review of interpretations and recent applications. *Journal of Applied Microbiology*, *119*(5), 1207–1218. https://doi.org/10.1111/jam.12902

Zelles, L., Palojɛarvi, A., Kandeler, E., Von Lutzow, M., Winter, K., & Bai, Q. Y. (1997). Changes in soil microbial properties and phospholipid fatty acid fractions after chloroform fumigation. *Soil Biology and Biochemistry*, *29*(9–10), 1325–1336. https://doi.org/10.1016/s0038-0717(97)00062-x